IAU Colloquium 164: Radio Emission from Galactic and Extragalactic Compact Sources
ASP Conference Series, Vol. 144, 1998
J. A. Zensus, G. B. Taylor, & J. M. Wrobel (eds.)

Magnetic Fields in AGN

J. F. C. Wardle
Physics Department, Brandeis University, Waltham, MA 02254, U.S.A.

Abstract. We review VLBI polarization results. In particular, we discuss the a) "shock in jet paradigm", b) the orientation of the magnetic field in jets as a function of optical identification, c) rotation measure and Faraday dispersion measurements as a probe of the narrow line region, and d) future directions of polarization observations. Results we emphasize are i) there is still a strong correlation between optical L/C ratio or EW and magnetic field orientation in the jets of blazars, even for high redshift weak-lined objects, ii) observed rotation measures are much smaller than expected from the properties of the NLR, except for some CSS sources. Also iii) a faint boundary layer or sheath (with a parallel magnetic field) has been observed around the jet of the weak-lined blazar 1055+018, and iv) circular polarization has been detected for the first time in the jets of 3C 84 and 3C 279.

1. The "Shock in Jet" Paradigm

It is now fairly widely accepted that the bright emission knots in the radio jets of AGNs are associated with relativistic shocks (Marscher & Gear 1985; Hughes, Aller, & Aller 1985). Such shocks have clear signatures in VLBI polarization images, since the compression enhances the transverse components of the underlying magnetic field, leading to polarization (electric vectors) either parallel or orthogonal to the jet, depending on the strength of the shock and of any component of the magnetic field parallel to the jet axis.

If the underlying parallel field component is weak or absent, as appears to be the case in BL Lac objects (Gabuzda et al. 1994), then the electric vectors in the shock are parallel to the jet, and the fractional polarization is *higher* in the knot than in the inter-knot regions (see 1055+018 , Attridge et al., these Proceedings, p. 159). If the parallel field component is strong, as in many quasars (Cawthorne et al. 1993), then the electric vectors in the shock are orthogonal to the jet, and the fractional polarization is *lower* in the knot than in the inter-knot regions (see 3C 345, Wardle et al. 1994; and 3C 273, Ojha et al., these Proceedings, p. 127). A sufficiently strong shock can always overwhelm the parallel field component, as appears to be the case in the quasar 3C 279 (see Homan et al., these Proceedings, p. 123), and in the innermost knots in other quasars observed at high enough resolution (Leppänen, Zensus, & Diamond 1995). Interestingly, the inner jet of the BL Lac object OJ 287 exhibited a parallel magnetic field, at least during 1996 (see Ojha et al., these Proceedings, p. 127).

VLBI polarization images are therefore a critical test of the shock paradigm, and in general they support it. They also permit direct measurement of important physical quantities such as the shock strength (Wardle et al. 1994).

As higher quality polarization images from the VLBA become available, we find a rich variety of polarization behaviors that are not so easily fit by such a simple model, and examples abound in these Proceedings. In general the magnetic field is a tracer of the underlying hydrodynamics of the jets, showing the effects of oblique shocks, boundary layer interactions, instabilities, shear, confinement, turbulence, and cloud collisions *inter alia*, whose manifestations are often much more easily seen (if not interpreted) in the polarization images than the total intensity images.

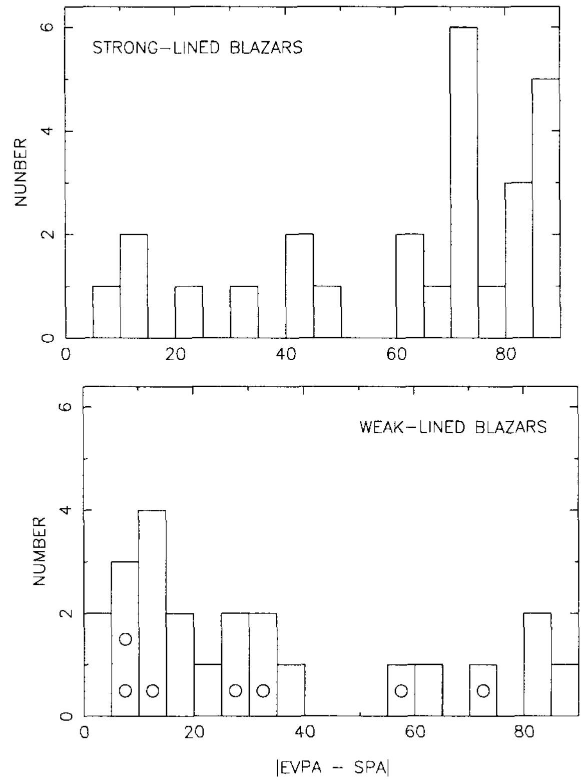

Figure 1. Magnetic field orientation in the jets of strong-lined and weak-lined blazars. See text for definitions. Weak-lined objects at $z > 0.5$ are indicated by circles.

2. The Orientation of Magnetic Fields in the Jets

The first clear result from VLBI polarimetry was the difference in magnetic orientation in the jets of sources identified as BL Lac objects and those identified as quasars (Cawthorne et al. 1993). While superficially indicating a simple distinction by optical identification, it raises difficulties for high redshift "BL Lac objects". These objects have emission line luminosities far higher than normal elliptical galaxies, and comparable to some quasars at low redshift. The division between BL Lac objects and quasars is conventionally set at 5 Å rest-frame equivalent width (EW). Some authors (e.g., Antonucci 1993) have argued that this is a meaningless division (leading to a possible time varying classification, among other things), and that they are all "blazars" with a wide range of line-to-continuum ratios. VLBI polarization can shed light on the problem.

In Figure 1 we show the angle between the polarization electric vectors (EVPA) and the local structural position angle of the jet (SPA) for strong-lined blazars (EW $>$ 5Å$(1+z)$, upper panel) and weak-lined blazars (EW $<$ 5Å$(1+z)$,

https://doi.org/10.1017/S0252921100044717 Published online by Cambridge University Press

lower panel). These include all objects for which the alignment is known at the present time, and include most of the sources with detectable jet polarization in the Pearson-Readhead (1988) and 1 Jy BL Lac samples (Kühr & Schmidt 1990). See also Pushkarev & Gabuzda (these Proceedings, p. 165).

The tendency for the net magnetic field orientation to be parallel to the jet in strong-lined objects and orthogonal to the jet in weak-lined objects still holds. Though there are plenty of exceptions in both cases (and sources such as 3C 279 and OJ 287 change orientation with distance from the core), the two distributions differ at > 99% significance level. Of particular interest are the high redshift ($z > 0.5$) weak-lined objects, marked with circles. Despite having luminous emission lines, they still tend to exhibit "BL Lac-like" behavior (5 objects) rather than "quasar-like" behavior (2 objects). It is also interesting that the weak-lined object with an almost perfectly aligned parallel field is in fact Mrk 501 at a redshift of only $z = 0.033$ (Aaron et al., in preparation).

There are many possible reasons for alignments other than 0° or 90°. These include oblique shocks, unresolved wiggles in the local jet direction, residual Faraday rotation, and turbulence scales not much smaller than the jet diameter. The quasar 4C 71.07 has a long and rather straight jet, and dual wavelength observations made by Hutchison & Cawthorne (these Proceedings, p. 125) show that the observed misalignment of 30° over much of the length of its jet cannot be attributed to Faraday rotation.

If the parallel component of the magnetic field is generated by a small transverse velocity gradient due to boundary layer interactions with the ambient medium (Cawthorne et al. 1993), then the important parameter may be the ratio of the density of the surrounding medium to the jet kinetic luminosity. This may be roughly proportional to the equivalent width of the emission lines or to the line to continuum ratio, which would be consistent with Figure 1.

The source 1055+018 ($z = 0.888$) is particularly interesting in this respect, since it lies almost exactly on the 5Å boundary. A snapshot observation showed a strongly polarized jet with a well aligned transverse magnetic field throughout. But a recent deep observation by Attridge et al. (these Proceedings, page 159) shows a sheath-like structure surrounding the jet, with a *parallel* magnetic field. It is possible that many or all jets would exhibit such a sheath, if observed with sufficient sensitivity, and that the apparent magnetic field orientation in lower dynamic range images is determined mainly by the relative brightnesses of the sheath and the spine. This picture is reminiscent of the model for FR I jets on kpc scales developed by Laing (1996).

3. Faraday Rotation and Dispersion, and the Narrow Line Region

The frequency agility of the VLBA has permitted Faraday rotation measurements to become straightforward, either between IFs in a single band to detect very large RMs, or between different bands for more modest RMs. This has been greatly aided by the excellent and quasi-logarithmic u-v coverage of the array. This permits pseudo scaled-array observations, so that a uniform weighted image at C band, for instance, has almost the same beam and similar effective u-v coverage as a naturally weighted image at X band. (For the same reasons, one can now make depolarization and spectral index maps of good fidelity.)

https://doi.org/10.1017/S0252921100044717 Published online by Cambridge University Press

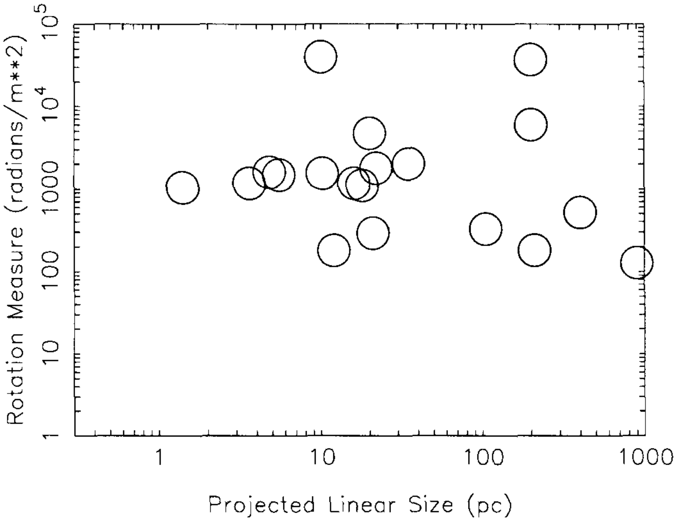

Figure 2. Rotation Measure as a function of projected distance from the VLBI core.

Parsec scale radio jets are presumably embedded in the region of narrow optical line emitting gas (NLR) in AGNs, which extends from about a parsec to at least several hundred parsecs from the nucleus. Faraday rotation maps at milliarcsecond resolution can give information about the distribution and properties of this gas on linear scales that are inaccessible to optical spectroscopy. Typical parameters quoted for the narrow-line clouds are densities $n \approx 10^3 - 10^5$ cm^{-3}, temperatures $\approx 10^4$K, random velocities $\approx$ a few hundred km/sec, and small volume filling factors $\approx 10^{-3}$ (e.g., Osterbrock 1993). What is not known is the magnetic field strength in the clouds, or their size.

Arguments based on equipartition arguments or shock models suggest magnetic fields $B \approx 10^{-3} - 10^{-4}$ G. As a bench mark, consider a cloud of diameter 1 pc, and a uniform magnetic field. Then the rms rotation measure of such a cloud is $RM(1pc) = 1/\sqrt{3} \times 8.1 \times 10^5 nBl \approx 10^{4.5} - 10^{7.5}$ rad m^{-2}. This is in contrast to observed RMs which are in the range 100 to 10^4 rad m^{-2}, as has been pointed out by many authors (e.g. Rudnick & Jones 1983; O'Dea 1989), who also discuss some possible solutions to the problem.

VLBA observations are starting to shed light on this (and to exacerbate it). Even before dual wavelength observations were made, it was clear that for most blazars the parsec scale polarization was rotated by less than a radian, or else the alignments seen in Figure 1 (mainly at λ6 cm) would be completely washed out. This corresponds to a $RM < 300(1+z)^2$ rad m^{-2} at the source.

There are many dual- or multi-wavelength observations of Faraday rotation reported in these Proceedings. These include contributions by Aaron, Wardle, & Roberts (3C 309.1, page 105), Flatters (3C 119, page 109), Hutchison & Cawthorne (4C 71.07, page 125), Lüdke et al. (3C 147, page 183, and 3C 216, page 185), Taylor, Venturi, & Udomprasert (OQ 172, page 113), Mantovani et al.

https://doi.org/10.1017/S0252921100044717 Published online by Cambridge University Press

(1741+279, page 65), Homan et al. (3C 279, page 123), and Ojha et al. (3C 273, OJ 287 page 127).

First some caveats. We shall not consider the RMs observed for VLBI core components. In the inhomogeneous jet model (Blandford & Königl 1979), the position of the "core" is at the $\tau = 1$ surface, which moves out with increasing wavelength. Thus the line of sight through any Faraday screen changes with wavelength, making the apparent RM difficult to interpret. Faraday rotation internal to the emitting region may also occur, but can be distinguished by deviations from a λ^2 rotation law for rotations $> 45°$. The mean RM over a VLBI image may include contributions from our Galaxy and from any intracluster medium etc., but RM gradients on the scale of milliarcseconds must occur in the AGN. Ideally, we want to measure the mean RM, its gradient, its beam-to-beam fluctuations, and the depolarization rate, as a function of distance from the core. All of these give useful (and different) information for constructing a model of the Faraday screen.

In Figure 2 we show a plot of $|RM|$ versus projected distance from the VLBI core for all sources for which at least dual wavelength observations have been made. The RMs have all been multiplied by $(1+z)^2$ to put them in the source frame. The most striking feature is simply the enormous range of RMs found on parsec scales. These range from 40,000 rad m^{-2} for OQ 172 to only a few hundred rad m^{-2} for 3C309.1 , 4C 71.07, and 1741+279. In only a few sources are the RMs comparable with the simple theoretical estimate above. These are OQ 172, 3C 119, 3C 147 and 3C 216, all of which are "Compact Steep Spectrum" (CSS) sources, for which there is other radio evidence for a dense medium surrounding the jets (e.g. Fanti et al. 1990). But it should be noted that in OQ 172, the RM drops to only 2000 rad m^{-2} at a distance of 35 pc from the core (Taylor et al., these Proceedings, page 113), and in 3C 216 the large RM is associated with a sharp bend or disruption in the jet and is much smaller closer to the core (Lüdke et al., these Proceedings, page 185). It should also be noted that where large RMs are detected, there is some coherence from beam to beam. This means that scale for magnetic field reversals is not smaller than the beam (these would also depolarize the radio emission), i.e. , the ambient magnetic field is partially ordered on scales of parsecs to tens of parsecs.

In the majority of sources, especially the blazars, there is essentially no evidence of the expected Faraday rotation (several of the points in Figure 2 are from high frequency observations, and are almost certainly upper limits). If the magnetic field is tangled on scales much smaller than a parsec, then the mean RM along a line of sight is reduced, but the radio emission will still be depolarized unless the scale of tangling is $\ll 10^{15}$ cm. We suggest instead that a crucial parameter is the covering factor of the narrow-line clouds. This is not well determined for many sources but is thought to be only a few percent (e.g. Netzer & Laor 1993). It is likely that almost *no* line of sight intercepts a narrow-line cloud. The observed RMs therefore reflect the properties of the inter-cloud medium, whose parameters are essentially unknown. A second factor is that in blazars the line of sight makes a small angle to the jet. If the visible jet is embedded in a much broader outflow that excludes the narrow-line clouds and is also Faraday thin, then this might explain both the small RMs observed in blazars, and the difference between blazars and CSS sources.

4. New Directions

The excellent feeds and sensitivity of the VLBA have enabled reliable polarization observations to be made at the shortest wavelengths. λ7 mm images of 3C 120 are shown by Gómez et al. (these Proceedings, page 119) and of BL Lac at many epochs by Denn & Mutel (these Proceedings, page 169). The CMVA, operating at λ3.5 mm, has made successful test runs detecting polarized fringes between many antennas, including on transatlantic baselines. We have demonstrated that the polarized fringes can be properly calibrated (Wardle et al. 1996), and images will appear soon. In principle there is no reason why polarization VLBI cannot be carried out at even shorter wavelengths. The only problem is limited sensitivity. Such observations probe the magnetic field structure near the base of jets, perhaps in the region where they first "turn on" at a standing shock (Marscher, these Proceedings, page 25). They may also set limits on Faraday rotation and depolarization in the broad-line region, which could be enormous if the broad-line clouds are magnetically confined (Rees 1987).

Comparably high resolution at longer wavelengths can be obtained by space VLBI. The VSOP antenna is equipped with dual circularly polarized feeds at each wavelength, and many polarization observations have been proposed. The next step in space VLBI—the ARISE mission—is described by Ulvestad & Linfield (these Proceedings, page 397). It proposes a VLBA scale antenna, which will have far greater sensitivity than VSOP.

As a dedicated array, the VLBA can pursue the monitoring of rapidly variable radio sources. Six epochs of monitoring 13 strongly polarized highly variable sources at intervals of two months at 15 and 22 GHz are described by Ojha et al. (these Proceedings, page 127). Changes in both core and jet components are observed between epochs, and for the first time it is possible to follow the evolution of outbursts, their spectrum, and their magnetic field in some detail. Equally exciting and more theoretically challenging, are the observations at VLBI resolution of intraday variability in 4 BL Lac objects presented by Gabuzda, Kochanev & Kollgaard (these Proceedings, page 265), and by Kochanev & Gabuzda (these Proceedings, page 273). They find changes in polarization over a few hours, confirmed by simultaneous observations with the VLA, without noticeable changes in total intensity. They interpret the polarization changes as being intrinsic to the source, perhaps due to extremely rapid evolution of shocks.

Finally, a very important new result is the detection of circular polarization at 15 GHz in the jets of 3C 84 and 3C 279 by Homan et al. (these Proceedings, page 123). Since these observations were part of a monitoring program, they have been able to show these detections are completely repeatable. Although circularly polarized feeds are a less than ideal way of detecting circular polarization, the superb characteristics of the VLBA permit detections at a level of a few tenths of a percent locally, if great care is exercised. Circular polarization can be due to the intrinsic circularly polarized component of synchrotron radiation ($\sim 1/\gamma$ in a uniform field, where γ is the Lorentz factor of the radiating particles). If this is the case, then the charge of the radiating particles can only be of one sign, since electrons and positrons gyrate in opposite directions. However, especially at high frequencies, only a few reversals in the line of sight component of the magnetic field render the intrinsic circular polarization very small. A second source of circular polarization is Faraday conversion of linear polarization

https://doi.org/10.1017/S0252921100044717 Published online by Cambridge University Press

to circular by low energy relativistic electrons in the emitting region (Jones & O'Dell 1977). This *linear* birefringence depends on the square of the charge on the particles, and is therefore the same for electrons, positrons, or a mixture of the two. Jones (1988) has shown that for a wide range of jet models, it is in fact difficult to avoid generating significant circular polarization by this mechanism. If the charge of the low energy particles is of only one sign, then there must also be internal Faraday rotation. Thus a signature of an electron-positron jet is the presence of Faraday conversion *without* Faraday rotation.

This is thought to be the case for 3C 279, where the circular polarization occurs in a component with strong linear polarization and no detectable Faraday rotation. In 3C 84, where the linear polarization is everywhere negligible, such an argument cannot be made, and the intrinsic mechanism cannot be ruled out. But for many sources, circular polarization observations offer a unique way to distinguish an electron-proton jet from an electron-positron jet, and to probe the low energy end of the relativistic particle spectrum.

Acknowledgments. I thank Denise Gabuzda for contributing unpublished results to Figure 1, and many other contributors to these Proceedings for communicating results in advance of the meeting. This work has been supported by NSF Grants AST 92-24848 and AST 95-29228, and NASA Grant NGT-51658. The National Radio Astronomy Observatory is a facility of the National Science Foundation, operated under a cooperative agreement by Associated Universities, Inc.

References

Antonucci, R. R. J. 1993. *ARA&A*, **31**, 473–521.

Blandford, R. D., & Königl, A. 1979. *ApJ*, **232**, 34–48.

Cawthorne, T. V., et al. 1993. *ApJ*, **416**, 519–535.

Fanti, R., et al. 1990. *A&A*, **231**, 333–346.

Gabuzda, D. C., et al. 1994. *ApJ*, **435**, 140–161.

Hughes, P. A., Aller, H. D., & Aller, M. H. 1985. *ApJ*, **298**, 301–315.

Jones, T. W., & O'Dell, S. L. 1977. *ApJ*, **214**, 522–539.

Jones, T. W. 1988. *ApJ*, **332**, 678–695.

Kühr, H., & Schmidt, G. D. 1990. *AJ*, **99**, 1–6.

Laing, R. A. 1996. In *Energy Transport in Radio Galaxies and Quasars*, eds. P. E. Hardee, A. H. Bridle, & J. A. Zensus (San Fransico: ASP), 241–252.

Leppänen, K. J., Zensus, J. A., & Diamond, P. J. 1995. *AJ*, **110**, 2479–2492.

Marscher, A. P., & Gear, W. K. 1985. *ApJ*, **298**, 114–127.

O'Dea, C. P. 1989. *A&A*, **210**, 35–41.

Osterbrock, D. E. 1993. *ApJ*, **404**, 551–562.

Pearson, T. J., & Readhead, A. C. S. 1988. *ApJ*, **328**, 114–142.

Rees, M. J. 1987. *MNRAS*, **228**, 47P–50P.

Rudnick, L., & Jones, T. W. 1983. *AJ*, **88**, 518–526.

Wardle, J. F. C., et al. 1994. *ApJ*, **437**, 122–135.

Wardle, J. F. C., et al. 1996. In *Millimeter-VLBI Science Workshop*, eds. R. Barvainis & R. B. Phillips (Cambridge: MIT), 63–67.